Fluid Phase Equilibria 329 (2012) 22–31

Contents lists available at SciVerse ScienceDirect

Fluid Phase Equilibria

journal homepage: www.elsevier.com/locate/fluid

An efficient algorithm for the calculation of phase envelopes of fluid mixtures

Sergio E. Quiñones-Cisneros [a], Ulrich K. Deiters [b,*]

[a] Instituto de Investigaciones en Materiales, Universidad Nacional Autónoma de México. Apdo. Postal 70-360, México D.F. 04510, Mexico
[b] Institute of Physical Chemistry, University of Cologne, Luxemburger Str. 116, D-50939 Köln, Germany

ARTICLE INFO

Article history:
Received 19 February 2012
Received in revised form 25 May 2012
Accepted 29 May 2012
Available online 7 June 2012

Keywords:
Fluid phase equilibrium
Calculation
Algorithm
Equation of state
Helmholtz energy density

ABSTRACT

The criteria of fluid phase equilibrium can be expressed in terms of derivatives of the Helmholtz energy density, which takes component densities (concentrations) as its natural variables. The resulting formulation is very symmetric, avoids shortcomings of other approaches, and leads to a very efficient computer algorithm for the calculation of phase envelopes of multicomponent mixtures.

The new algorithm does without inverting the equation of state (calculate the density from pressure and temperature) at each iteration step, and thus achieves a significant acceleration of phase diagram computations with noncubic equations of state. The estimation of initial values for the iteration is reduced to a 1-dimensional search problem even for multicomponent mixtures.

1. Introduction

The task we are considering in this article is the computation of the composition of a fluid phase in equilibrium with a fluid phase of given composition at a fixed temperature, plus the determination of the equilibrium pressure.

The problem is as old as the techniques of distillation and extraction, and many solution strategies been proposed during the last century. The thermodynamic conditions of phase equilibrium were already concisely formulated by Gibbs and his followers by the end of the 19th Century [1]. While already van der Waals and his school realized that the application of these conditions to a real-gas equation of state could lead to a uniform and consistent description of vapor–liquid and liquid–liquid equilibria [2], this became practically feasible only after electronic computers became available to the public around 1960. Still, it takes more than merely a fast computer to solve the systems of nonlinear equations which describe the equilibrium between fluid phases: The convergence of iterative schemes is not always granted, and sometimes is too slow for comfort. The need for fast and reliable algorithms became even more pressing with the arrival of noncubic equations of state and multidimensional corresponding states schemes.

The work of Michelsen [3,4] is considered an important landmark in the "art" of computing fluid phase equilibria. It summarizes the thermodynamic conditions of equilibrium and phase stability, and proposes highly efficient strategies to determine the equilibrium compositions. Michelsen's work is based on the analysis of the Gibbs energy surface proposed by Baker et al. [5].

We will show in this work that an analysis of another surface, namely the Helmholtz energy density surface, can lead to even more efficient algorithms. Incidentally, the usage of this surface leads to a rather "symmetric" and esthetically satisfying formulation of the phase equilibrium conditions.

2. Theory

2.1. Phase equilibrium and stability criteria

In order to have an equilibrium between two phases, here denoted as $'$ and $''$, it is necessary that they have the same temperature and the same pressure; furthermore, the chemical potentials of each component must have the same value in the coexisting phases:

$$\begin{aligned} T' &= T'' \\ p' &= p'' \\ \mu_i' &= \mu_i'' \quad i = 1, \ldots, N \end{aligned} \tag{1}$$

In addition, it is necessary that the phases fulfill some stability criteria, namely

$$\frac{C_V}{T} > 0, \tag{2}$$

* Corresponding author. Tel.: +49 221 470 4543; fax: +49 221 470 4900.
E-mail address: ulrich.deiters@uni-koeln.de (U.K. Deiters).

0378-3812/$ – see front matter © 2012 Elsevier B.V. All rights reserved.
http://dx.doi.org/10.1016/j.fluid.2012.05.023

which is the condition of thermal stability,

$$\left(\frac{\partial^2 A}{\partial V^2}\right)_T > 0 \tag{3}$$

which is the condition of mechanical stability, and, for binary mixtures,

$$\left(\frac{\partial^2 G_m}{\partial x_1^2}\right)_{p,T} > 0. \tag{4}$$

Eq. (4) is often called the criterion of diffusion stability. It can be shown that mixtures — with the exception of azeotropic mixtures — reach the limit of diffusion stability before reaching the mechanical stability limit, Eq. (3).

These stability criteria of pure fluids and azeotropic mixtures on one side, and general mixtures on the other, have been known for a long time. Still, it may strike one as odd that two different criteria, involving two different thermodynamic potentials, must be used for practically the same phenomenon.

For a multicomponent mixture, the diffusion stability criterion requires the Hessian matrix of the molar Gibbs energy to be positive definite, i.e.,

$$\boldsymbol{v}\cdot\boldsymbol{G}\cdot\boldsymbol{v} > 0 \quad \text{with}$$

$$\boldsymbol{G} = \begin{pmatrix} \frac{\partial^2 G_m}{\partial x_1^2} & \frac{\partial^2 G_m}{\partial x_1 \partial x_2} & \cdots & \frac{\partial^2 G_m}{\partial x_1 \partial x_{N-1}} \\ \frac{\partial^2 G_m}{\partial x_2 \partial x_1} & \frac{\partial^2 G_m}{\partial x_2^2} & \cdots & \frac{\partial^2 G_m}{\partial x_2 \partial x_{N-1}} \\ \vdots & \vdots & \ddots & \vdots \\ \frac{\partial^2 G_m}{\partial x_{N-1} \partial x_1} & \frac{\partial^2 G_m}{\partial x_{N-1} \partial x_2} & \cdots & \frac{\partial^2 G_m}{\partial x_{N-1}^2} \end{pmatrix}, \tag{5}$$

for any non-zero vector $\boldsymbol{v}$ in composition space, while the derivatives of $G_m(\boldsymbol{x}; p, T)$ are computed at constant pressure and temperature. The molar Gibbs energy, however, can have more than one value for a given pressure, and is therefore not a true function. Hence Eq. (5) is not really well-defined. Furthermore, because of this multiplicity, the criterion is not sufficient to ensure global stability, as even mechanically unstable phases can result in a positive definite $\boldsymbol{G}$ [6,7].

This is not merely a matter of mathematical esthetics. Because of the peculiar behavior of $G_m(\boldsymbol{x}; p, T)$, it is not generally possible to search for two-phase regions by looking at the local curvature of the Gibbs energy surface. This problem is illustrated in Fig. 1 for a simple case of a two-component mixture: At high temperatures, in the vicinity of the critical curve of the system, the Gibbs energy curve $G_m(x_1)$ exhibits the "classical" S-shape with two inflection points (spinodal states) and a region of concave curvature between them (case A). At low temperatures, however, the Gibbs energy "function" has got three branches. If the subroutine for the Gibbs energy calculation always returns the lowermost (=the most stable) value, the concave region may be inaccessible (case B). But it may happen that no concave region exists at all (case C).

Provided that the condition of thermal stability, Eq. (2), is satisfied everywhere, one way to avoid the problems associated with the use of G_m is formulating the stability criterion in terms of the molar Helmholtz energy, $A_m(\boldsymbol{x}, V_m; T)$: the Hessian of $A_m(\boldsymbol{x}, V_m; T)$ has to be positive definite:

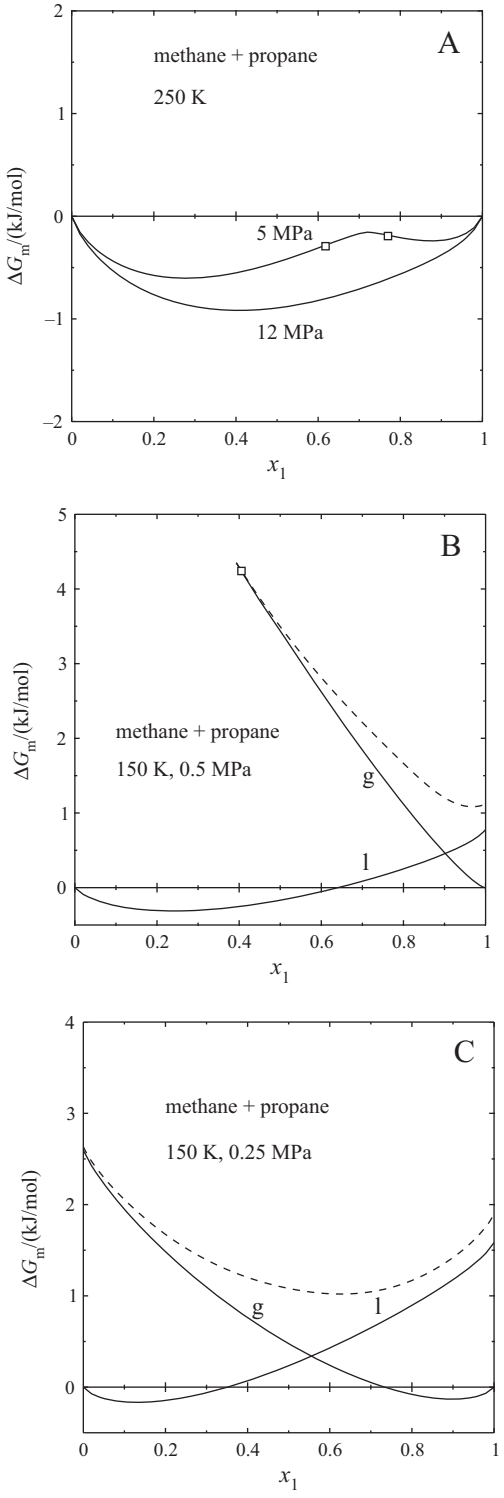

Fig. 1. Gibbs energy G_m as a function of mole fraction x_1 for the system {methane (1) + propane (2)}, calculated with the Peng–Robinson equation of state. For clarity, a linear function $x_1 G_{m,1} + x_2 G_{m,2}$ has been subtracted. —: mechanically stable branch, - - -: mechanically unstable branch, and □: spinodal.

$\boldsymbol{v}\cdot\boldsymbol{A}\cdot\boldsymbol{v} > 0$ with

$$\boldsymbol{A} = \begin{pmatrix} \frac{\partial^2 A_m}{\partial x_1^2} & \frac{\partial^2 A_m}{\partial x_1 \partial x_2} & \cdots & \frac{\partial^2 A_m}{\partial x_1 \partial x_{N-1}} & \frac{\partial^2 A_m}{\partial x_1 \partial V_m} \\ \frac{\partial^2 A_m}{\partial x_2 \partial x_1} & \frac{\partial^2 A_m}{\partial x_2^2} & \cdots & \frac{\partial^2 A_m}{\partial x_2 \partial x_{N-1}} & \frac{\partial^2 A_m}{\partial x_2 \partial V_m} \\ \vdots & \vdots & \ddots & \vdots & \vdots \\ \frac{\partial^2 A_m}{\partial x_{N-1} \partial x_1} & \frac{\partial^2 A_m}{\partial x_{N-1} \partial x_2} & \cdots & \frac{\partial^2 A_m}{\partial x_{N-1}^2} & \frac{\partial^2 A_m}{\partial x_{N-1} \partial V_m} \\ \frac{\partial^2 A_m}{\partial x_1 \partial V_m} & \frac{\partial^2 A_m}{\partial x_2 \partial V_m} & \cdots & \frac{\partial^2 A_m}{\partial x_{N-1} \partial V_m} & \frac{\partial^2 A_m}{\partial V_m^2} \end{pmatrix}, \tag{6}$$

and $\boldsymbol{v}$ denoting a non-zero vector in ($\boldsymbol{x}$, V_m) space.

Now this criterion has the problem of combining variables of different units and magnitudes, potentially leading to large asymmetries (depending on the system of units chosen) and causing numerical difficulties.

The problem can be circumvented by defining a scaling factor that makes V_m dimensionless. This, however, introduces an arbitrariness into thermodynamic calculations which should rather be avoided.

In this work we propose another, esthetically more satisfying solution to the problem, namely a "symmetric" formulation of phase stability and equilibrium criteria.

2.2. Isochoric thermodynamics

Instead of treating the $N-1$ independent mole fractions, x_1, x_2, …, x_{N-1} and the molar volume, V_m, as primary variables, we propose to treat the total volume, V as fixed and use the amounts of substance, n_1, n_2, …, n_N. This is equivalent to introducing component densities or concentrations, ρ_1, ρ_2, …, ρ_N, as primary variables:

$$\rho_i = \frac{n_i}{V} = \frac{x_i}{V_m} \tag{7}$$

This approach may therefore be called "isochoric thermodynamics" or "density-based thermodynamics". It is, of course, not a new concept; for instance, Sengers and Levelt Sengers [8] used it in 1978 to discuss critical phenomena in fluid mixtures.

The re-conversion to molar volumes and mole fractions is accomplished by

$$\rho = \sum_i \rho_i = \frac{1}{V_m}$$
$$x_i = \frac{\rho_i}{\rho} \tag{8}$$

The total differential of the Helmholtz energy is

$$\mathrm{d}A = -S\,\mathrm{d}T - p\,\mathrm{d}V + \sum_{i=1}^{N} \mu_i\,\mathrm{d}n_i. \tag{9}$$

Because of V = const, the second term on the right-hand side is zero. Dividing by V then yields

$$\mathrm{d}\Psi \equiv \mathrm{d}\left(\frac{A}{V}\right) = -\frac{S_m}{V_m}\,\mathrm{d}T + \sum_{i=1}^{N} \mu_i\,\mathrm{d}\rho_i, \tag{10}$$

where $\Psi \equiv A/V$ is the Helmholtz energy density, which was proposed by Sengers and Levelt Sengers as primary thermodynamic potential [8]. Evidently, the densities ρ_i are natural variables of Ψ.

From Eq. (10) one can see that the chemical potentials can be written as

$$\mu_i = \left(\frac{\partial \Psi}{\partial \rho_i}\right)_{V,T,\rho_{j\neq i}}, \tag{11}$$

and therefore the phase equilibrium criterion of equal chemical potentials becomes

$$\left(\frac{\partial \Psi'}{\partial \rho_i}\right) = \left(\frac{\partial \Psi''}{\partial \rho_i}\right), \quad i = 1, \ldots, N. \tag{12}$$

For clarity, we omit the constant properties in the partial derivatives here and in the following equations, as they are always the same.

In order to derive an expression for the pressure in the density-based formulation, we combine the definition of the Gibbs energy,

$$G = A + pV, \tag{13}$$

and the relation

$$G = \sum_{i=1}^{N} n_i \mu_i \tag{14}$$

to obtain

$$-p = \frac{1}{V}\left(A - \sum_{i=1}^{N} n_i \mu_i\right). \tag{15}$$

Inserting Eq. (11) and the definition of Ψ yields

$$p = -\Psi + \sum_{i=1}^{N} \left(\frac{\partial \Psi}{\partial \rho_i}\right) \rho_i. \tag{16}$$

Hence the equal-pressure criterion, $p' = p''$, becomes

$$\sum_{i=1}^{N} \left(\frac{\partial \Psi''}{\partial \rho_i}\right) \rho_i'' - \sum_{i=1}^{N} \left(\frac{\partial \Psi'}{\partial \rho_i}\right) \rho_i' = \Psi'' - \Psi'. \tag{17}$$

or, using Eq. (12),

$$\sum_{i=1}^{N} \left(\frac{\partial \Psi}{\partial \rho_i}\right) (\rho_i'' - \rho_i') = \Psi'' - \Psi' \equiv \Delta\Psi. \tag{18}$$

Using vector notation, the phase equilibrium conditions Eqs. (12) and (18) can finally be summarized as

$$\begin{aligned} &\boldsymbol{\mu}' = \boldsymbol{\mu}'' \;\Rightarrow\; \nabla\Psi'' = \nabla\Psi' \\ &p' = p'' \;\Rightarrow\; \nabla\Psi\cdot\Delta\boldsymbol{\rho} = \Delta\Psi \quad \text{with} \quad \Delta\boldsymbol{\rho} = \boldsymbol{\rho}'' - \boldsymbol{\rho}' \end{aligned} \tag{19}$$

This represents a system of $N+1$ equations for the unknown densities $\boldsymbol{\rho}''$ and $\rho' = \sum \rho_i'$.

The geometric interpretation of these equations is that, under isothermal conditions, $\Psi(\boldsymbol{\rho})$ defines a curved surface in $\boldsymbol{\rho}$ space. $\nabla\Psi(\boldsymbol{\rho})$ represents the slopes of this surface with respect to the densities of all mixture components. The support plane of $\Psi(\boldsymbol{\rho})$ at the location $\boldsymbol{\rho}'$, i.e., the (hyper)plane tangent to the surface, can then be specified by

$$L(\boldsymbol{\rho}, \boldsymbol{\rho}') = \Psi' + \sum_{i=1}^{N} \left(\frac{\partial \Psi'}{\partial \rho_i}\right)(\rho_i - \rho_i') = \Psi' + \nabla\Psi'\cdot(\boldsymbol{\rho} - \boldsymbol{\rho}'). \tag{20}$$

Evidently, the pressure criterion in Eq. (19) can be written as

$$L(\boldsymbol{\rho}'', \boldsymbol{\rho}') = \Psi'' \tag{21}$$

which means that the point of the Ψ surface representing the coexisting phase, $\Psi'' = \Psi(\boldsymbol{\rho}'')$, is on the same support plane: the support plane is a double tangent plane to the Ψ surface.

2.3. Generation of initial values

Eq. (19) represents the system of equations that has to be solved in order to find the component densities of coexisting phases. These equations are nonlinear and can generally be solved by iterative techniques only. Then, however, it is necessary to provide good initial values for the iteration.

This can be accomplished by considering the total differential of Ψ, Eq. (10), which we write now for the isothermal case as

$$\mathrm{d}\Psi = \sum_{i=1}^{N} \left(\frac{\partial \Psi}{\partial \rho_i} \right) \mathrm{d}\rho_i = \nabla \Psi \, \mathrm{d}\boldsymbol{\rho}. \tag{22}$$

Integration of this equation yields

$$\Delta \Psi = \int_{\Omega} \nabla \Psi \, \mathrm{d}\boldsymbol{\rho}, \tag{23}$$

where Ω denotes an arbitrary path in $\boldsymbol{\rho}$ space. We are of course interested in a path that runs from the locus of the phase with the given composition to the locus of the yet unknown equilibrium phase. Comparison of this equation with the pressure criterion in Eq. (19) shows that the latter can be regarded as the special case of the path integral for adjacent phases:

$$\int_{\boldsymbol{\rho}'}^{\boldsymbol{\rho}''} \nabla \Psi \, \mathrm{d}\boldsymbol{\rho} \rightarrow \nabla \Psi \cdot \Delta \boldsymbol{\rho} \tag{24}$$

In the general case, however, the path integral value will differ from its linear approximation, and the difference can be expected to depend on the size of $\Delta\boldsymbol{\rho}$. We therefore write the path integral expression to 2nd order as

$$\int_{\boldsymbol{\rho}'}^{\boldsymbol{\rho}''} \nabla \Psi \, \mathrm{d}\boldsymbol{\rho} = \nabla \Psi \cdot \Delta \boldsymbol{\rho} + \frac{\lambda}{2} (\Delta \boldsymbol{\rho})^2 = \Delta \Psi. \tag{25}$$

Calculating the gradient of this equation, i.e., the outer product with the nabla operator, gives

$$\nabla \cdot \nabla \Psi \cdot \Delta \boldsymbol{\rho} + \nabla \Psi + \lambda \, \Delta \boldsymbol{\rho} = \nabla (\Delta \Psi). \tag{26}$$

The left-hand side of this equation contains the Hessian matrix of the Helmholtz energy density:

$$\boldsymbol{\Psi} \equiv \nabla \cdot \nabla \Psi = \begin{pmatrix} \dfrac{\partial^2 \Psi}{\partial \rho_1^2} & \dfrac{\partial^2 \Psi}{\partial \rho_1 \partial \rho_2} & \cdots & \dfrac{\partial^2 \Psi}{\partial \rho_1 \partial \rho_N} \\ \dfrac{\partial^2 \Psi}{\partial \rho_2 \partial \rho_1} & \dfrac{\partial^2 \Psi}{\partial \rho_2^2} & \cdots & \dfrac{\partial^2 \Psi}{\partial \rho_2 \partial \rho_N} \\ \vdots & \vdots & \ddots & \vdots \\ \dfrac{\partial^2 \Psi}{\partial \rho_N \partial \rho_1} & \dfrac{\partial^2 \Psi}{\partial \rho_N \partial \rho_2} & \cdots & \dfrac{\partial^2 \Psi}{\partial \rho_N^2} \end{pmatrix}. \tag{27}$$

With regard to the right-hand side of Eq. (26), we observe that Ψ' does not depend on $\boldsymbol{\rho}''$, nor Ψ'' on $\boldsymbol{\rho}'$. If the gradient is taken with respect to $\boldsymbol{\rho}''$, one of the terms cancels,

$$\nabla(\Delta\Psi) = \nabla_{\rho''} \Psi'' - \underbrace{\nabla_{\rho''} \Psi'}_{=0} = \nabla_{\rho''} \Psi'', \tag{28}$$

and therefore Eq. (26) reduces to

$$\boldsymbol{\Psi} \, \Delta \boldsymbol{\rho} = -\lambda \, \Delta \boldsymbol{\rho}. \tag{29}$$

Evidently, this is an eigenvalue equation for $\Delta\boldsymbol{\rho}$. As $\Delta\boldsymbol{\rho}$ is a vector that points from the locus of the given phase to the locus of the equilibrium phase, the meaning of this equation is that one has to follow one of the eigenvectors of $\boldsymbol{\Psi}$ in order to arrive at the equilibrium phase; most likely, the eigenvector associated to the lowermost eigenvalue will be the correct one.

Eq. (29) is true for adjacent equilibrium phases, i.e., phases of such similar compositions that the path integral can be replaced by a 2nd-order approximation. This is certainly the case for phase equilibria in the vicinity of critical points [9], but Eq. (29) is also applicable far away from critical points as long as the phase compositions are not too different [7].

In the general case, the path from the fixed phase to the other phase can be broken up into a sequence of short paths, and Eq. (29) applied to each these paths — with the consequence that $\boldsymbol{\Psi}$ and hence the direction of the relevant eigenvector change along this path. The path will therefore appear curved in $\boldsymbol{\rho}$ space.

It is perhaps interesting to attempt a geometric interpretation: The matrix $\boldsymbol{\Psi}$ represents the local curvature of the $\Psi(\boldsymbol{\rho})$ surface, expressed in terms of the densities $\boldsymbol{\rho}$. The eigenvalues of $\boldsymbol{\Psi}$ represent principal curvatures in the directions of the eigenvectors. By following an eigenvector-defined path over the $\Psi(\boldsymbol{\rho})$ surface, we align our search with the "local landscape". Such a search path, when originating from a locally stable phase, has previously been called "lowest ascendant path" [9].

For a stable or at least metastable phase, the local curvature must be convex, and this implies that all eigenvalues are positive [9]. Conversely, if at least one eigenvalue is negative, the phase is unstable; this constitutes a criterion for phase stability.

If we move from one equilibrium phase, $\boldsymbol{\rho}'$ to the other one, $\boldsymbol{\rho}''$, along the double tangent plane, $L(\boldsymbol{\rho}, \boldsymbol{\rho}')$, the curvature along our path is zero. If the movement is made along the Ψ surface, which lies above the tangent plane, there must be a region of concave curvature, and consequently at least one eigenvalue will become negative there. Monitoring the lowermost eigenvalue is therefore a good way to recognize two-phase regions.

A formal proof and a more detailed discussion of stability criteria based on the principal curvatures of the Hessians of thermodynamic potentials is already available elsewhere [7,9] and will be the subject of a forthcoming publication.

2.4. Calculation of Ψ

For completeness' sake, we give here the equation which relates $\Psi = A/V = \rho A_\mathrm{m}(\boldsymbol{\rho}\,; T)$:

$$A_\mathrm{m}(\boldsymbol{x}, V_\mathrm{m}; T) = \sum_{i=1}^{N} x_i (G^{\ominus}_{\mathrm{m},i}(T) + RT \, \ln x_i) - RT - \int_{V^{\ominus}_\mathrm{m}}^{V_\mathrm{m}} p(\boldsymbol{x}, V_\mathrm{m}; T) \, \mathrm{d}V_\mathrm{m} \tag{30}$$

The derivation of this equation can be found in the literature (e.g., [10], Sect. 4.2). Here $p^{\ominus} = RT/V^{\ominus}_\mathrm{m}$ denotes a reference state at such a large volume that here the ideal-gas law holds. The $G^{\ominus}_{\mathrm{m},i}$ are the Gibbs energies of the pure components i of the mixture in that state. In phase equilibrium calculations (unless chemical reactions have to be accounted for) all these reference terms cancel and therefore need not be considered here.

$p(\boldsymbol{x}, V_\mathrm{m}\,; T)$ is an arbitrary pressure-explicit equation of state of the fluid state. Usually such an equation is created by choosing an appropriate pure-fluid equation of state and making its substance-specific parameters composition-dependent.

Splitting the equation of state into an ideal and a residual part,

$$p = \frac{RT}{V_\mathrm{m}} + p^\mathrm{r}, \tag{31}$$

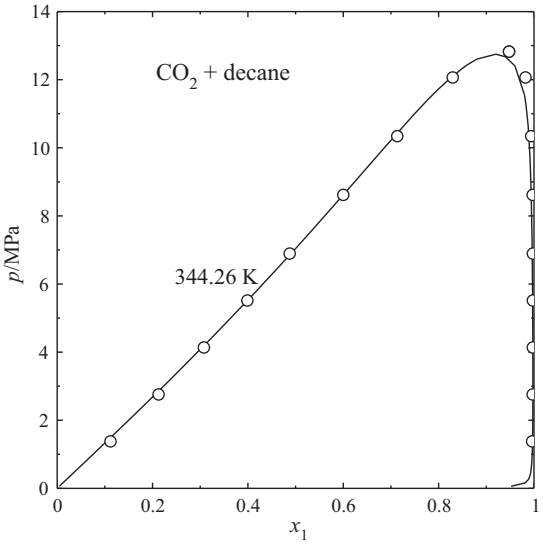

Fig. 2. Isothermal phase diagram of the {carbon dioxide (1) + decane (2)} system at 344.26 K. —: computed with the Peng–Robinson equation of state and ○: experimental data [20].

and converting from molar volumes and mole fractions to molar densities then leads to

$$\Psi(\boldsymbol{\rho};T) = \sum_{i=1}^{N}\rho_i\left(G^{\ominus}_{\mathrm{m},i}(T) + RT\,\ln\left(\frac{\rho_i}{\rho^{\ominus}}\right)\right) - RT\rho + \rho\int_0^{\rho}\frac{p^{\mathrm{r}}(\boldsymbol{\rho};T)}{\rho^2}\,\mathrm{d}\rho. \quad (32)$$

The integral in this equation can be evaluated analytically or numerically, depending on the complexity of the equation of state.

The derivatives of Ψ which are required for $\nabla\Psi$ and $\boldsymbol{\Psi}$ (Eqs. (19) and (27)) can be obtained most conveniently by numerical differentiation; usually two steps of Romberg's or Ridder's method are sufficient (see for example [10], Sect. A.8). Alternatively, analytical differentiation can be used, preferably by means of computer algebra.

We defer further programming considerations to Section 4 and look first at representations of phase equilibria and search paths on $\Psi(\boldsymbol{\rho})$ surfaces.

3. Examples of phase diagram calculations

3.1. Two-phase equilibria

Fig. 2 shows the "classical view" of an isothermal phase diagram of the fluid mixture {carbon dioxide + decane} at 344.26 K. At this temperature, carbon dioxide is supercritical. Consequently, the phase boundary has the typical loop shape with a binary critical point. This example was calculated with the Peng–Robinson equation of state (with the mixing rules proposed by its authors) [11] by means of the *ThermoC* program [12].

Fig. 3 displays the corresponding $\Psi(\rho_1,\rho_2)$ diagram.[1] The pseudocolors indicate the "height", i.e., the Ψ value at each location. The phase boundary, several connodes, and the critical point are marked in the diagram. Close to the left side of the diagram, at the decane axis, there is an elevation, a region of concave curvature, which owes its existence to the vapor–liquid equilibrium of decane.

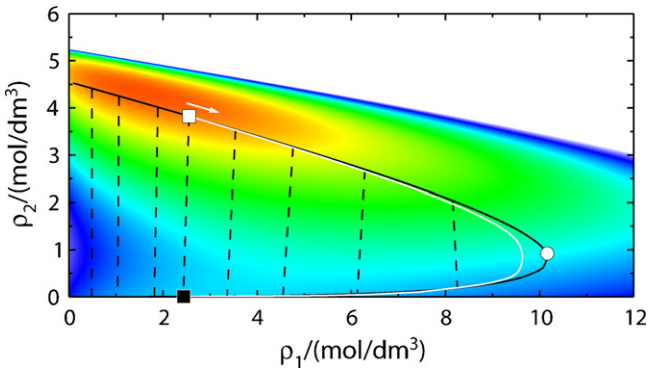

Fig. 3. $\Psi(\rho_1,\rho_2)$ diagram of the {carbon dioxide (1) + decane (2)} system at 344.26 K, calculated with the Peng–Robinson equation of state. —: phase boundary, - - -: connodes, ○: critical point, □, ■: starting and final point of a search for initial values, white curve: eigenvector path; pseudocolors: Ψ value (red = low, blue = high, white = undefined; grayscale: black = low, white = high or undefined). A linear function was subtracted from Ψ in order to make best use of the color gamut. (For interpretation of the references to color in this figure legend, the reader is referred to the web version of the article.)

The white area in the upper right part of the diagrams represents the forbidden region, i.e., the region where the molar volume would be less than the covolume of the equation of state.

We note in passing that (ρ_1, ρ_2) diagrams have a long tradition in statistical thermodynamics; they are sometimes called *Meijer diagrams*. In the original work [13] they appear as (x_1, x_2) diagrams of ternary lattice gases with $x_0 + x_1 + x_2 = 1$, where x_0 represents a "hole species". The mole fractions of a lattice gas with a fixed lattice size correspond, of course, to the ρ_i of this work.

Fig. 3 also illustrates the eigenvector-based search algorithm for initial values. If a liquid phase with $x_1 = 0.4$ is given, the search follows the path indicated by the eigenvector belonging to the lowermost eigenvalue. As can be seen in the figure, this path practically runs through the equilibrium state at the other end of the connode, i.e., the equilibrium vapor phase.

Fig. 4 shows the behavior of the lowermost eigenvalue along the path indicated in Fig. 3: The path originates at the locus of the liquid phase (which is stable, $\lambda > 0$), runs through an unstable region, and arrives at a stable region again, where it passes through the locus of the vapor phase.

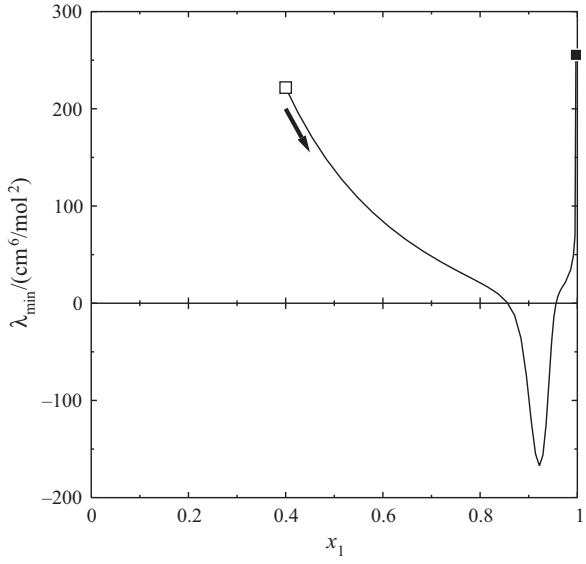

Fig. 4. Computation of a connode of the {carbon dioxide (1) + decane (2)} system at 344.26 K: eigenvalue along the path shown in Fig. 3.

[1] For better visual effect, a linear function has been subtracted so that the corners of the triangular map are at zero.

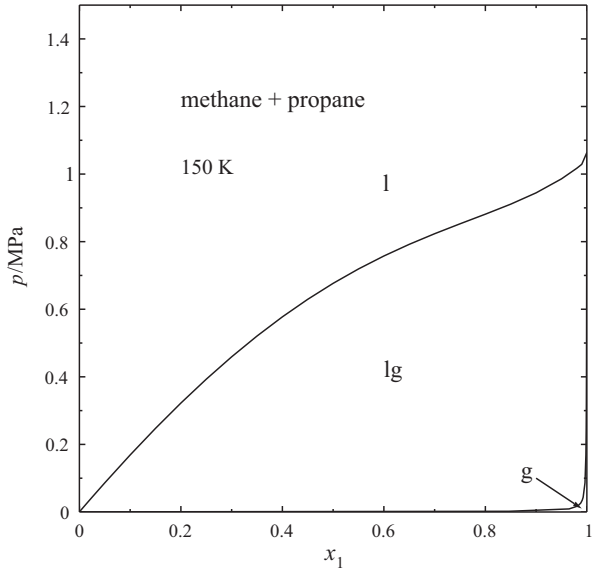

Fig. 5. Isothermal phase diagram of the {methane (1) + propane (2)} system at 150 K. —: computed with the Peng–Robinson equation of state.

It turns out, therefore, that the eigenvector search reduces the problem of locating the coexisting phase to a 1-dimensional search — regardless of the dimensionality of the problem (=the number of components).

Figs. 5 and 6 show subcritical and supercritical, respectively, phase diagrams of the {methane + propane} system, again calculated with the Peng–Robinson equation of state. Figs. 7 and 8 display the corresponding Ψ surfaces, with the phase envelopes and some connodes marked. In the subcritical case, the two-phase region stretches from one coordinate axis to the other, and the connodes rotate by 90° to accommodate this transition. In the supercritical case, the phase envelope is terminated by a binary critical point.

In the subcritical case, there is a very deep "canyon" in the Ψ surface which misleads the search algorithm: The search along the first eigenvector, i.e., the one belonging to the lowermost eigenvalue, λ_1, follows the canyon and thus goes astray. In such a case it is advisable to search along another eigenvector and, when the

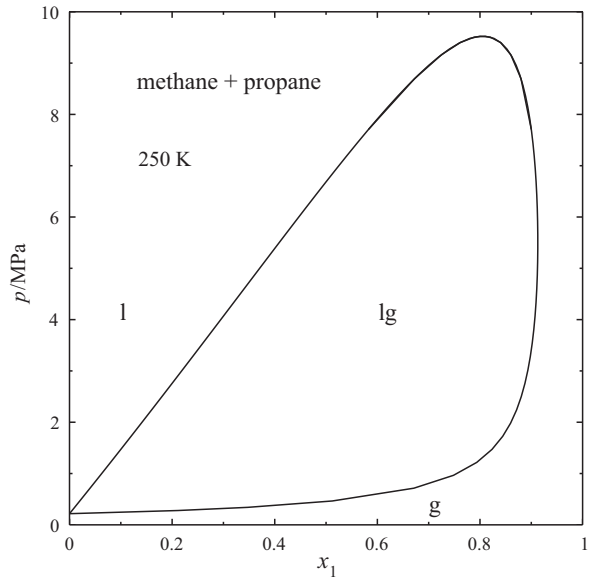

Fig. 6. Isothermal phase diagram of the {methane (1) + propane (2)} system at 250 K. —: computed with the Peng–Robinson equation of state.

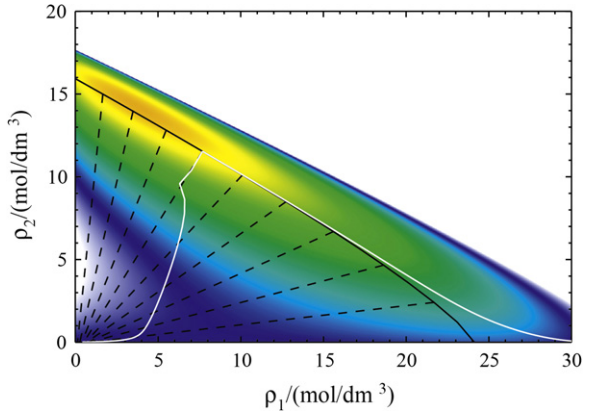

Fig. 7. $\Psi(\rho_1, \rho_2)$ diagram of the {methane (1) + propane (2)} system at 150 K, calculated with the Peng–Robinson equation of state. For an explanation of the symbols and colors see Fig. 3.

associated eigenvalue passes through a minimum or λ_1 gets negative, to switch back to the first eigenvector. The resulting path has been indicated in Fig. 7: it runs through the other end of the connode. Alternatively, one can start the search for the phase equilibrium at the vapor side of the connode; this search succeeds immediately. In the supercritical case, the search along the first eigenvector finds the other end of the connode without any problems (see Fig. 8).

The failure of the first search attempt on the liquid side has got a physical reason: The search algorithm locates adjacent equilibrium phases first, and it turns out that the "canyon" is the region where at lower temperatures or for larger alkane chain lengths a liquid–liquid phase separation will take place.

3.2. Three-phase equilibria

Fig. 9 shows an isothermal phase diagram of the system {carbon dioxide + hexadecane} at 313.15 K, computed with the Peng–Robinson equation. The system exhibits a liquid–liquid phase split superimposed on the vapor–liquid equilibrium.

This diagram was computed with the new algorithms. A run started at the lower left corner of the diagram (l_1g equilibrium) moves to the right side (l_2g) without any problems; only the "wriggle" of the bubble point curve indicates the presence of a liquid–liquid phase split (l_1l_2). A run of the program started at high pressures finds this phase split and follows it down into the

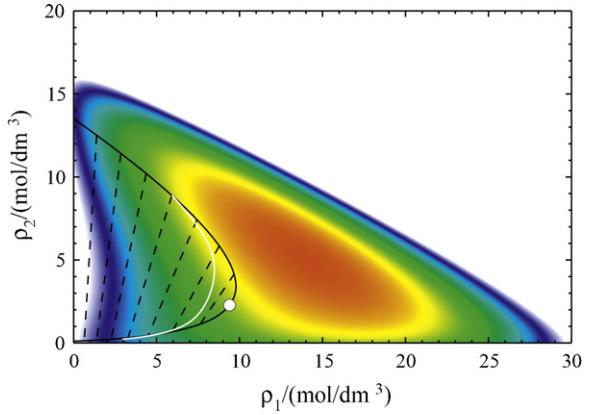

Fig. 8. $\Psi(\rho_1, \rho_2)$ diagram of the {methane (1) + propane (2)} system at 250 K, calculated with the Peng–Robinson equation of state. For an explanation of the symbols and colors see Fig. 3.

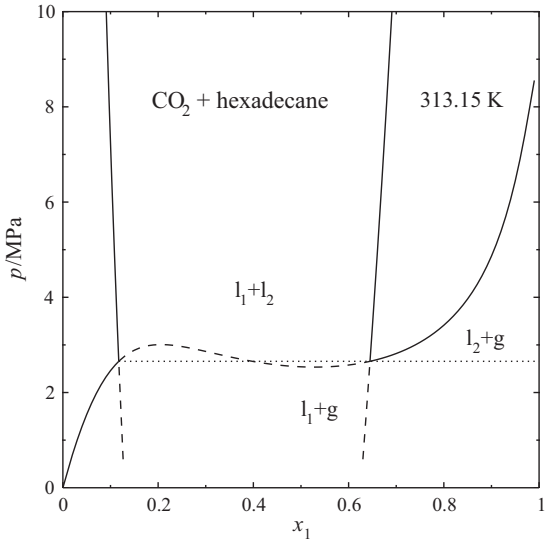

Fig. 9. Isothermal phase diagram of the system (carbon dioxide + hexadecane) at 313.15 K, calculated with the Peng–Robinson equation of state. —: stable phase boundaries, - - -: metastable phase boundaries, and ···: three-phase state llg. With the present graphical resolution, the dew point curve practically coincides with the diagram frame.

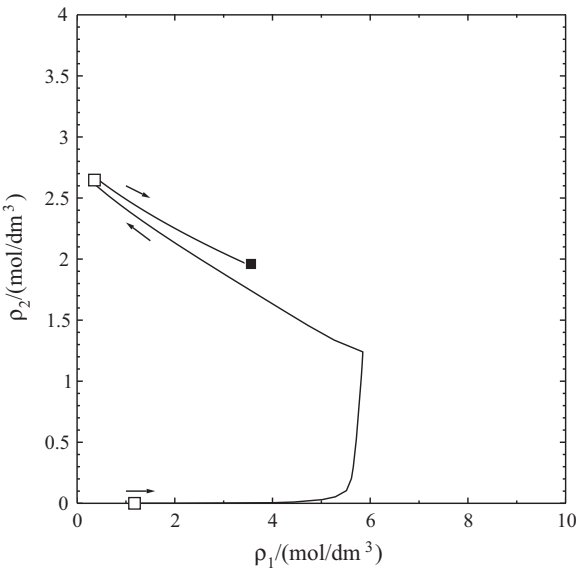

Fig. 11. Search paths for the {carbon dioxide (1) + hexadecane (2)} system at 313.5 K at the pressure of the three-phase equilibrium. □: starting points (liquid phase l_2 or gas phase and ■: end point (liquid phase l_1.

metastable region. The l_1l_2g three-phase state is obtained from the intersections of these curves.

Fig. 10 shows the corresponding Meijer diagram. The overall topology is very similar to that of the {carbon dioxide + decane} case, but now the "valley" along the high-density border of the diagram is deeper and has become a "canyon", which has a concave portion along its rim; this gives rise to the liquid–liquid phase split. The connodes of the three-phase state form a triangle; the gas phase corresponds to the lower vertex.

Fig. 11 shows the paths taken during the initialization phase of the phase equilibrium algorithm, for equilibrium phases in the vicinity of the three-phase state:

1. The eigenvector path starting at the liquid phase l_2 is almost straight and practically runs into l_1. This can evidently be considered as a case of "adjacent" phases.
2. The eigenvector path starting at the gas phase is at first almost horizontal (vanishing hexadecane concentration), then turns upwards as the compressed carbon dioxide becomes able to dissolve more and more of the alkane. A sharp bend in the path indicates a switch from one eigenvector to the other (the algorithm follows the eigenvector with the lowest eigenvalue). Directly at this bend, the eigenvectors are degenerated, and no clear direction can be given. This is an unusual complication. Still, the path continues, passes the l_1 state very closely, and finally runs almost exactly into l_2. The slight inaccuracies seen in Fig. 11 are partly due to the degeneration point, and partly to following the eigenvector paths with a finite step size. Depending on where the search is terminated and the root finder is invoked, either the l_1g or the l_2g equilibrium is computed.

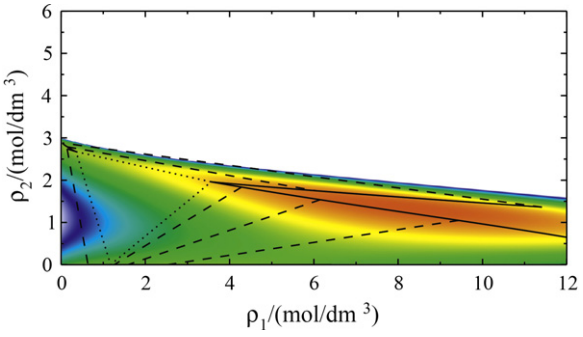

Fig. 10. $\Psi(\rho_1, \rho_2)$ diagram of the {carbon dioxide + hexadecane} system at 313.15 K. ···: connodes of the three-phase state. See Fig. 3 for an explanation of the colors and the other lines.

Since in a $\Psi(\boldsymbol{\rho})$ surface the coexisting phase are always separated by unstable regions ($\lambda_1 < 0$), but are themselves stable ($\lambda_1 > 0$), the middle phase of a three-phase state must be near to a maximum of the eigenvalue. This fact can eventually be used to locate three-phase states.

4. Programming considerations and application

4.1. Orthobaric densities

It should be noted that, in the system of equations Eq. (19), the pressure does not appear explicitly, and the orthobaric densities ρ' and ρ'' are obtained as sums of the component densities: There is no need to invert the equation of state (i.e., calculate the density from pressure and temperature) at each iteration step.[2]

This advantage is paid for by having one more unknown in the main iteration: For a binary mixture, finding a phase equilibrium in a $G_m(x_1)$ representation requires a search along one mole fraction (1 unknown variable), whereas a search of $\Psi(\rho_1, \rho_2)$ evidently involves two variables. But this may still save time, for the inversion of equations of state, especially noncubic ones, can be computationally costly (see Section 4.3). Furthermore, the additional unknown is not felt much in calculations for multicomponent systems.

Another point worth noting is that no ambiguities exist within the phase equilibrium calculation. With the conventional method, where the pressure is specified and the phase volume calculated, there may be more than one solution. In such a case, one has to select the volume which gives the lowest Gibbs energy, and this

[2] This feature is shared by the algorithm of Mikyška and Firoozabadi [14], which also uses densities, but is based on a different concept. The work came to our attention after our algorithm had been developed.

means additional computation steps. With the method described here, such ambiguities cannot appear.

4.2. Outline of the algorithm

From Eq. (19), the object function for the phase diagram calculation can be defined:

$$\boldsymbol{y} = \begin{pmatrix} y_1 \\ \vdots \\ y_n \\ y_{n+1} \end{pmatrix} = \begin{pmatrix} \dfrac{\partial \Psi''}{\partial \rho_1} - \dfrac{\partial \Psi'}{\partial \rho_1} \\ \vdots \\ \dfrac{\partial \Psi''}{\partial \rho_n} - \dfrac{\partial \Psi'}{\partial \rho_n} \\ \Psi'' - \Psi' - \sum \dfrac{\partial \Psi'}{\partial \rho_i}(\rho_i'' - \rho_i') \end{pmatrix} \tag{33}$$

$\boldsymbol{y}$ must vanish if $\boldsymbol{\rho}'$ and $\boldsymbol{\rho}''$ belong to coexisting fluid phases. The implementation of Eq. (33) for solving with a nonlinear root finder, e.g., the Marquardt–Levenberg algorithm, is straightforward.

The new phase equilibrium algorithm can be summarized as follows:

(A) Initialization
  (1) Read the composition of the fixed phase, the temperature, and an estimate for the equilibrium pressure p.
  (2) Check the stability of the fixed phase (e.g., by computing the density vector, $\boldsymbol{\rho}'$, and the eigenvalues of its Hessian, $\boldsymbol{\Psi}$).
    If the fixed phase is unstable (i.e., at least one eigenvalue is negative), change the pressure until a stable state is obtained. Lowering the pressure toward zero will always lead to a stable state. But if the fixed phase is supposed to be a liquid, it might be advisable to increase the pressure.
  (3) Set $\boldsymbol{\rho}'' := \boldsymbol{\rho}'$, and follow the path pointed out by the eigenvector belonging to the lowermost eigenvalue, λ_1, in the direction of decreasing eigenvalues, i.e., $\boldsymbol{\rho}'' := \boldsymbol{\rho}'' + \alpha\ \boldsymbol{u_1}$. A reasonable choice for the size of α is $0.1 \min|\rho_i''/u_{1,i}|$ (assuming that $\boldsymbol{u_1}$ is a unit vector). Repeat this several times.
    If the eigenvalue begins to increase again without ever having become negative or if the search path runs into illegal density values, go back and try another eigenvector. If its associated eigenvalue passes through a minimum or λ_1 becomes negative, switch to the first eigenvector and continue to move in the direction of decreasing eigenvalues.
    If the lowest eigenvalue gets negative and then positive again, a two phase region has been located. In this case ...
  (4) Continue to follow the eigenvector path, but monitor the norm of the object function, $\boldsymbol{y^2}$, for a minimum.
(B) Calculation of equilibrium states
  (1) At this minimum, run the nonlinear root finder. Print the result.
  (2) Change the temperature or the composition of the fixed phase.
  (3) Extrapolate initial values for the nonlinear root finder, e.g., by polynomial extrapolation.
  (4) Go to (B.1).

Concerning (A): This is a relatively slow process. It should be run at the start of the program only, or if the extrapolation of initial values fails.

Concerning (A.4): One might save time by going to (B.1) as soon as the eigenvalue turns positive again, but sometimes this is too soon for the root finder.

Table 1
CPU time required to compute a supercritical isotherm of the {carbon dioxide + decane} system. PR: Peng–Robinson equation of state and XD: Xiang–Deiters.

Equation of state	t/s	
	G_m-based	Ψ-based
PR	0.09	0.10
XD	2.45	0.55
PC-SAFT	10.50	0.36

Concerning (B.1): If the estimates for $\boldsymbol{\rho}'$ and $\boldsymbol{\rho}''$ are located at different sides of the concave region, and $\boldsymbol{\rho}''$ is close to a minimum of $\boldsymbol{y^2}$, convergence is very likely.

Our derivations in Section 2.3 assumed that the starting point of the search part is known. But if the initial state is not specified in terms of densities, $\boldsymbol{\rho}'$, but mole fractions, $\boldsymbol{x'}$, its overall density has to be estimated from the pressure. If the initial state is supposed to be a liquid, even a more than slightly wrong pressure will usually not affect the density much. Of course, an initial pressure guess that is too far off the mark can "spoil the aim" of the initialization algorithm. But again, trying other eigenvectors than the one belonging to the lowermost eigenvalue may help.

4.3. Performance

Table 1 contains computing times for a single isotherm (about 40 equilibrium states) of our test system, {carbon dioxide + decane} at 344.26 K. The following equations of state were used:

1. Peng–Robinson (PR) [11]
   This is a cubic equation of state, for which highly efficient inverting methods are available. The mixing rules used were the ones proposed by its authors, i.e., 1-fluid theory based on Soave's function.
2. Xiang–Deiters (XD) [15]
   This is a noncubic equation based on a multidimensional corresponding states approach. Here the mixing rules of Plöcker et al. [16] were used.
3. PC-SAFT [17,18]
   This is a relatively complicated noncubic equation of states based on statistical thermodynamics. It contains special concentration-dependent functions.

The substance dependent parameters of these equations of state are listed in Tables 2–4.

The computations were carried out on a personal computer (Intel Xeon-type processor), using the *ThermoC* program package [12]. The reference calculation method was a program that solves G_m-based phase equilibrium conditions by means of a Marquardt–Levenberg subroutine.

Evidently, the new algorithm is not faster than the classical method if the equation of state can be rapidly inverted. But for

Table 2
Parameters of the Peng–Robinson of state used for the computation of the figures. T^*: characteristic temperature, v^*: characteristic volume, and ω: acentric factor. [The parameters in the original publication are $a_c = 8RT^*v^*$, $b = v^*$.]

Substance	T^*/K	v^*/(cm^3 mol^{-1})	ω
CH_4	140.15923	26.777108	0.01100
C_3H_8	271.69933	56.124099	0.15308
$C_{10}H_{22}$	453.80566	189.990843	0.48840
CO_2	223.49696	26.654121	0.22800
$CH_4 + C_3H_8$	176.03268	41.544759	
$CH_4 + C_{10}H_{22}$	151.65312	108.407434	
$C_3H_8 + C_{10}H_{22}$	294.92810	123.151630	
$CO_2 + C_{10}H_{22}$	185.65633	110.603760	

noncubic equations of state, significant CPU time savings can be achieved.

We note in passing that the Marquardt–Levenberg algorithm is not the world's fastest method for solving systems of nonlinear equations; instead, its strength is reliability (range of convergence) rather than speed. It is possible to speed up the calculations significantly with a dedicated Newton algorithm [19], but then the range of convergence may be smaller, especially for multicomponent mixtures.

It should be noted that azeotropy, the phenomenon of having two different phases with the same composition, becomes apparent only if mole fractions or mass fractions are used to measure phase compositions. But the liquid and the vapor phase of an azeotropic state have different molar volumes, and therefore different $\boldsymbol{\rho}$ vectors. Consequently, an algorithm based on $\boldsymbol{\rho}$ instead of $\boldsymbol{x}$ is not disturbed by azeotropy.

The new algorithms were found to work well in the immediate vicinity of critical points. As $\boldsymbol{\rho}' = \boldsymbol{\rho}''$ is true not only for a critical point, but also for a trivial solution of the phase equilibrium conditions, this case has to be suppressed. But in calculations of isopleths of supercritical mixtures, the equilibrium algorithm was found to move through the critical region without any sign of convergence problems.

That the phase equilibrium algorithm avoids the calculation of phase volumes for pressure has the interesting consequence that it is possible to follow phase equilibria into the negative-pressure domain. An example is given in Fig. 12, which shows isopleths of the {methane + propane + n-decane} system with a methane mole fraction of 0.9 and various C_3/C_{10} ratios. For mixtures with a high decane content, the isopleths run upwards to high pressures and change their character from vapor–liquid to liquid–liquid equilibrium [9]. For a small decane content, the isopleths may pass through a minimum which can even lie at negative pressures. While such states are often regarded as "science fiction", they play a role in studies of phase stability or nucleation phenomena. Furthermore, following the isopleth through the minimum to positive pressures is a straightforward way to locate the liquid–liquid phase split at low temperatures.

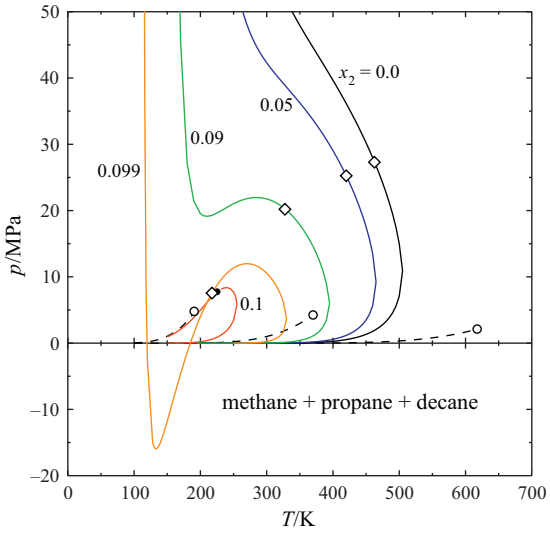

Fig. 12. Isopleths of the ternary system {methane (1) + propane (2) + decane (3)}, calculated with the Peng–Robinson equation of state, for $x_1 = 0.90$. Solid curves: isopleths (parameter: x_2), - - -: vapor pressure curves, ○: pure-fluid critical points, ●: mixture critical point, and ◊: isopiestic points (where the coexisting phases have the same molar densities).

5. Conclusion

Using the Helmholtz energy density $\Psi(\boldsymbol{\rho}, T)$ with densities $\boldsymbol{\rho}$ as arguments instead of the Gibbs energy, $G_m(\boldsymbol{x}; p, T)$ or the Helmholtz energy $A_m(\boldsymbol{x}, V_m; T)$ leads to a very symmetric and esthetically satisfying formulation of the thermodynamic conditions of phase equilibrium. The formulation avoids problems caused by variables of different dimension.

It should be noted that the phase equilibrium or stability conditions for mixtures can also be applied to pure fluids. In particular, the stability criterion is that the Hessian of the Helmholtz energy density, $\boldsymbol{\Psi}$, is positive definite, which means that all its eigenvalues are positive. For pure fluids this reduces to $\partial^2\Psi/\partial\rho^2 > 0$, which is equivalent to Eq. (3), the mechanical stability criterion.

The $\Psi(\boldsymbol{\rho}, T)$ surface of a fluid mixture has not got any discontinuities or ambiguities like the Gibbs energy surface. Consequently, the search for phase equilibrium regions can be based on an analysis of the local curvature. In particular, it can be shown that the eigenvectors of $\boldsymbol{\Psi}$ can be used to locate the coexisting phase of a given (fixed) phase. Even for a multicomponent mixture, the search for initial values for the phase equilibrium calculation is a 1-dimensional problem only.

The evaluation of the phase equilibrium conditions, which is a nonlinear problem usually requiring iterative solution methods, can be accomplished with $\Psi(\boldsymbol{\rho}, T)$ in such a way that there is no need to invert the equation of state (i.e., calculate the molar volumes from pressure and temperature). Especially with complicated noncubic equations, this can lead to a significant acceleration of computations.

The phase equilibrium algorithm proposed in this work is not affected by azeotropy, and it shows a remarkably robust convergence in the vicinity of critical points. The behavior of $\Psi(\boldsymbol{\rho}, T)$ near critical points and the direct calculation of critical states, however, require some special consideration. These topics will be discussed in a forthcoming article.

Table 3
Parameters of the Xiang–Deiters equation of state used for the computation of Table 1. T^*: characteristic temperature, v^*: characteristic volume, ω: acentric factor, and θ: asphericity parameter. The mixing rule for T^* of Plöcker, Knapp, and Prausnitz amounts to computing mole fraction averages of $T_{ij}^*(v_{ij}^*)^\nu$; here $\nu = 1$ was used.

Substance	T^*/K	v^*/(cm³ mol⁻¹)	ω	θ
CO_2	304.128	94.1189	0.225	2.38E−4
$C_{10}H_{22}$	617.7	609.0	0.489	1.65086E−3
$CO_2 + C_{10}H_{22}$	336.3302	359.0595		

Table 4
Parameters of the PC-SAFT equation of state used for the computation of Table 1. T^*: characteristic temperature of a chain segment, v^*: characteristic volume of a chain segment, and m: effective number of chain segments.

Substance	T^*/K	v^*/(cm³ mol⁻¹)	m
CO_2	169.21	6.81269	2.0729
$C_{10}H_{22}$	243.87	178.32	4.6627
$CO_2 + C_{10}H_{22}$	185.62879	12.322345	

Nomenclature

A	Helmholtz energy
G	Gibbs energy
N	number of components
n	amount of substance
p	pressure
S	entropy
T	temperature

V volume
x mole fraction
y object function (phase equilibrium criteria)
λ eigenvalue
μ chemical potential
ρ molar density
Ψ Helmholtz energy density

$\boldsymbol{x}$, $\boldsymbol{\rho}$, ... (lower-case bold symbols) vectors, with elements representing mixture components
$\boldsymbol{G}$, $\boldsymbol{\Psi}$, ... (upper-case bold symbols) Hessian matrices

Subscripts and superscripts
i belonging to mixture component i
m molar property
r residual property
$'$, $''$ phase indicators
$\ominus$ ideal-gas reference state

Acknowledgments

Inspiration by P.H.E. Meijer (Catholic University of America, Washington, D.C.), who introduced one of us (U.K.D.) to the critical phenomena of lattice gases, is gratefully acknowledged.

This work was carried out within a Mexican-German scientific exchange program, jointly supported by CONACyT (Consejo Nacional de Ciencia y Tecnología) and DFG (Deutsche Forschungsgemeinschaft). Complementary financial support was derived from the UNAM PAPIIT project IN115009.

References

[1] J.W. Gibbs, On the equilibrium of heterogeneous substances, in: R.G. van Name, H.A. Bumstead (Eds.), The Scientific Papers of J. Willard Gibbs, vol. 1: Thermodynamics, Dover Publications, New York, 1961, reprint of a book of 1906 containing articles originally published in 1876–1878.
[2] J.D. van der Waals, P. Kohnstamm, Lehrbuch der Thermodynamik in ihrer Anwendung auf das Gleichgewicht von Systemen mit gasförmig-flüssigen Phasen, vol. 1, Maas & van Suchtelen, Amsterdam, 1908.
[3] M.L. Michelsen, The isothermal flash problem. Part I. Stability, Fluid Phase Equilib. 9 (1982) 1–19.
[4] M.L. Michelsen, The isothermal flash problem. Part II. Phase-split calculation, Fluid Phase Equilib. 9 (1982) 21–40.
[5] L.E. Baker, A.C. Pierce, K.D. Luks, Gibbs energy analysis of phase equilibria, Soc. Pet. Eng. J. 22 (1982) 731–742.
[6] S.E. Quiñones-Cisneros, Fluid phase equilibria from minimization of the free energy, Master's Thesis, University of Minnesota, 1987.
[7] S.E. Quiñones-Cisneros, Critical behavior in fluid mixtures, Ph.D. Thesis, University of Minnesota, 1992.
[8] J.V. Sengers, J.M.H. Levelt Sengers, Critical phenomena in classical fluids, in: C.A. Croxton (Ed.), Progress in Liquid Physics, Wiley, Chichester, 1978 (Chapter 4).
[9] S.E. Quiñones-Cisneros, Barotropic phenomena in complex phase behaviour, Phys. Chem. Chem. Phys. 6 (2004) 2307–2313.
[10] U.K. Deiters, T. Kraska, High-Pressure Fluid Phase Equilibria — Phenomenology and Computation, Supercritical Fluid Science and Technology, Elsevier, Amsterdam, 2012.
[11] D.Y. Peng, D.B. Robinson, A new two-constant equation of state, Ind. Eng. Chem. Fundam. 15 (1976) 59–64.
[12] U.K. Deiters, *ThermoC* project homepage: http://thermoc.uni-koeln.de/index.html.
[13] P.H.E. Meijer, M. Napiórkowski, The three-state lattice gas as model for binary gas–liquid systems, J. Chem. Phys. 86 (1987) 5771–5777.
[14] J. Mikyška, A. Firoozabadi, A new thermodynamic function for phase-splitting at constant temperature, moles, and volume, AIChE J. 57 (2011) 1897–1904.
[15] H.-W. Xiang, U.K. Deiters, A new generalized corresponding-states equation of state for the extension of the Lee–Kesler equation to fluids consisting of polar and larger nonpolar molecules, Chem. Eng. Sci. 63 (2007) 1490–1496.
[16] U. Plöcker, H. Knapp, J.M. Prausnitz, Calculation of high-pressure vapor–liquid equilibria from a corresponding-states correlation with emphasis on asymmetric mixtures, Ind. Eng. Chem. Process Des. Dev. 17 (1978) 324–332.
[17] J. Gross, G. Sadowski, Application of perturbation theory to a hard-chain reference fluid: an equation of state for square-well chains, Fluid Phase Equilib. 168 (2000) 183–199.
[18] J. Gross, G. Sadowski, Perturbed-chain SAFT: an equation of state based on a perturbation theory for chain molecules, Ind. Eng. Chem. Res. 40 (2001) 1244–1260.
[19] U.K. Deiters, A modification of Newton–Raphson algorithm for phase equilibria calculations using numerical differentiation of the Gibbs energy, Fluid Phase Equilib. 19 (1985) 287–293.
[20] H.H. Reamer, B.H. Sage, Phase equilibria in hydrocarbon systems. Volumetric and phase behavior of the n-decane–CO_2 system, J. Chem. Eng. Data 8 (1963) 508–513.